Investigating the Theoretical Noise-Bandwidth Limits of Near-Terahertz Superconducting Heterodyne Mixers for Up-coming Far-Infrared Space Satellite Missions

B. -K. Tan[1], J-. H. Kim[1], A. Baryshev[2], and F. Boussaha[3]

[1]Department of Physics (Astrophysics), University of Oxford, OX1 3RH Oxford, United Kingdom.
[2]Kapteyn Astronomical Institute, University of Groningen 9747 AD, The Netherlands.
[3]LUX, Observatoire de Paris, Université PSL, Sorbonne Université, CNRS, 75014 Paris, France.

Abstract— We present the design and performance analysis of waveguide-based superconductor–insulator–superconductor (SIS) mixers employing niobium titanium nitride (NbTiN) transmission lines and tunnel junctions comprising niobium/aluminium oxide (Nb/AlO_x/Nb) or niobium/aluminium nitride (Nb/AlN/Nb) topologies. These superconducting quantum devices are developed to enable wideband heterodyne operation for next-generation far-infrared (FIR) space missions in the sub-terahertz regime. The mixer circuits are optimised for simultaneous broadband radio-frequency (RF) and intermediate-frequency (IF) operation using microstrip architectures that incorporate end-stub, end-loaded, and twin-junction tuning networks. Three-dimensional electromagnetic simulations, combined with quantum-mixing analyses, predict receiver noise temperatures approaching four times the quantum limit across 0.50–0.79 THz for the AlO_x-based design. The AlN-based variant further extends the RF coverage to 0.39–0.82 THz, satisfying the requirements of several proposed space missions while overlapping the Atacama Large Millimetre/sub-millimetre Array (ALMA) Bands 8 and extended Band 9. These simulated results demonstrate that NbTiN-based microstrip SIS mixers have the potential to deliver high sensitivity and wide instantaneous bandwidth at sub-terahertz frequencies, establishing them as strong candidates for next-generation space-borne and ground-based FIR observatories.

1. INTRODUCTION

The astronomical electromagnetic spectrum within the observable far-infrared (FIR) frequency range encompasses nearly half of the photon energy in the universe and contains numerous emission and absorption lines from atomic and molecular species, which can only be accessed through heterodyne spectroscopic observations. These observations are essential for understanding the kinematics and dynamics of these constituents, as well as the evolution of the interstellar medium, stars, and galaxies.

For FIR astronomical observations below 1.2 THz and above 0.1 THz, spanning the millimetre (mm) to sub-millimetre (sub-mm) range, it has become customary to employ superconductor–insulator–superconductor (SIS) heterodyne mixers as the primary ultra-sensitive coherent detectors. SIS mixers have demonstrated sensitivity approaching the quantum limit, with exceptionally low added noise across a wide radio-frequency (RF) and intermediate-frequency (IF) bandwidth [1, 2]. Consequently, eight of the ten observing bands of the Atacama Large Millimetre/sub-millimetre Array (ALMA) [3], one of the most important mm/sub-mm observatories currently in operation, are based on SIS mixer technology [4].

ALMA, together with other ground-based FIR observatories such as the James Clerk Maxwell Telescope (JCMT), the Large Millimetre Telescope (LMT), the Institut de Radioastronomie Millimétrique (IRAM) 30-metre telescope, the Northern Extended Millimetre Array (NOEMA), the Sub-millimetre Array (SMA), and many others, has enabled major advances in FIR astrophysics over the past few decades. However, their performance is fundamentally constrained by atmospheric water-vapour absorption, particularly above ∼0.4 THz, where atmospheric transmission decreases noticeably and severely limits the number of usable observing hours. Only about four high and dry sites on Earth can support observations above ∼0.4 THz: the Atacama Desert in northern Chile, the summit of Mauna Kea in Hawai'i, the Greenland summit, and the South Pole. Even at these sites, the availability of high-frequency observing time is strongly dependent on weather conditions, with accessibility decreasing rapidly at higher frequencies.

The 0.4–1.2 THz range covers three of the highest ALMA-defined frequency bands, namely Band 8 (0.385–0.5 THz), Band 9 (0.6–0.72 THz), and Band 10 (0.79–0.95 THz). Notably, frequency gaps exist above and below Band 9 due to significant atmospheric water-vapour absorption, which renders the sky nearly opaque for observations of certain important spectral lines e.g., the carbon monoxide (CO) $J = 5 \rightarrow 4$ transition line (0.57 THz) and many other astronomical water lines. However, these atmospheric limitations can be overcome using high-altitude balloon platforms and space-borne missions. For this reason, most above-atmosphere observatories employ heterodyne receivers whose lowest operational bands begin near 0.4 THz (comparable to ALMA Band 8) and extend to several terahertz. Beyond ∼1.2,THz, SIS receivers are generally replaced by hot-electron bolometer (HEB) mixers [5].

In this paper, we investigate the noise–bandwidth limitations of SIS mixers operating near the lower half of the 0.4–1.2 THz frequency range, using well-established niobium (Nb) tunnel junction technology with either aluminium oxide (AlO_x) or aluminium nitride (AlN) barriers [6, 7, 8]. In our design, the commonly used niobium (Nb) signal-carrying transmission line is replaced with a 400 nm thick niobium titanium nitride (NbTiN) line, which has a higher gap frequency of about 1.4 THz in contrast to 0.68 THz of Nb, thereby reducing transmission losses. The ground plane remains a thin 250 nm Nb layer.

This investigation is highly relevant to several upcoming and proposed FIR balloon-borne [9, 10, 11] and space-borne missions [12, 13, 14, 15, 16]. Specifically, the SIS detectors presented in this paper is designed to meet the noise–bandwidth requirements of the lowest-frequency channel of the Heterodyne Spectrometer Instrument (HSI) proposed for the Far-Infrared Spectroscopy Space Telescope (FIRSST, [17]), as well as the lowest SIS channel for the Light Emission Terahertz Observatory (LETO, [18]), a European Space Agency (ESA) M-class (M8) mission proposal.

Observations in this frequency range are also crucial for upcoming Event Horizon Telescope (EHT) campaigns, particularly through observations of the CO $J = 6 \rightarrow 5$ transition line (0.69 THz), which aim to produce faster and sharper images and videos of black holes [19, 20, 21]. The same frequency range is also relevant to forthcoming space-VLBI (very long baseline interferometry) missions focused on black holes such as the Black Hole Explorer [22], a NASA (National Aeronautics and Space Administration) Small Explorer (SMEX) missions proposal; and the Space-based High-resolution Array for Radio Astronomy and Physics (SHARP, [23]), another ESA-M8 mission proposal. Moreover, the same mixer designs can be utilised for a range of ground-based observatories, including the ALMA Wideband Sensitivity Upgrade (WSU) programme [24, 25] and other mm/sub-mm telescopes such as JCMT, GLT, and the up-coming large single-aperture mapping telescope such as Atacama Large Aperture Sub-Millimetre Telescope (AtLAST, [26]) and Large Sub-millimetre Telescope (LST) [27].

2. WIDEBAND HETERODYNE MIXER FOR SPACE-BORNE FIR MISSIONS

Here, we focus on the design of a waveguide-based SIS mixer operating around Band 9, using well-established waveguide-probe antenna [28] and Nb tunnel junction fabrication technology, with the exception of the NbTiN wiring layer, which has been shown to perform effectively in similar applications [29, 30]. To achieve wider noise–bandwidth performance, both at the RF and down-converted IF ranges, it is essential to understand the impact of the mixer's on-chip superconducting circuitry. This understanding enables optimal impedance matching (to minimise signal loss) and tuning of the junction's parasitic capacitances over the widest possible operational RF and IF bandwidths. Consideration of the dimensions of the radial-probe antenna, microstrip RF transformers, junction tuner circuits, RF chokes, bonding pads, and other on-chip components is crucial, as these elements may induce unwanted resonances within the operational bandwidth.

To achieve this, we model the ultra-broadband RF/IF SIS device using a three-dimensional (3-D) electromagnetic simulator, *Ansys*® High Frequency Structure Simulator (HFSS) [31], to account for all subtle effects that are often neglected. For heterodyne noise-temperature and conversion-gain predictions, we employ *SuperMix* [32, 33], a quantum-mixing software package based on Tucker's Quantum Mixing Theory, by importing the S-parameter matrix simulated from HFSS to ensure an accurate description of the mixer chip [34].

We have previously reported the design of ALMA–WSU Band 9 mixers capable of achieving a wide 20 GHz IF bandwidth covering the extended Band 9 range [35] from 0.58–0.74 THz (instead of the current ALMA-defined range of 0.6–0.72 THz), utilising primarily coplanar-waveguide (CPW) transmission lines on chip to reduce parasitic geometric capacitance observed at IF frequencies [36]. Further improvements to the RF bandwidth for ground-based observatories may not be practical due to limitations imposed by atmospheric water-vapour absorption. However, maximising the RF bandwidth is essential for future space-borne FIR missions, where reducing the number of

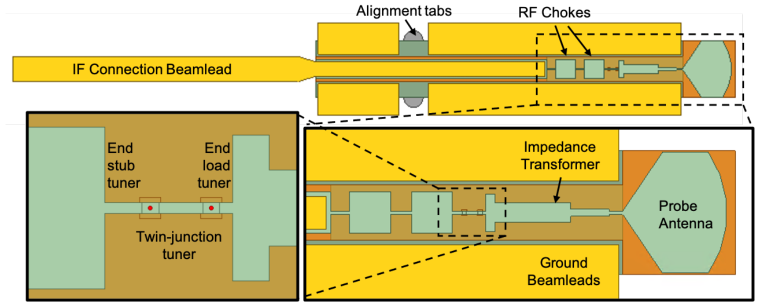

Figure 1: Layout of the microstrip SIS mixer chip. All on-chip circuit components are realised using microstrip transmission lines, except for the bonding pad that connects to the IF beam-lead. The inset illustrates the combination of a twin-junction, end-loaded, and end-stub tuner circuit used to achieve broadband RF performance of the mixer chip.

receivers and associated hardware is critical for minimising power consumption, mass, and volume constraints.

Almost all proposed up-coming space FIR missions incorporate HEB arrays for observations above 1.2 THz, taking advantage of the superior observing conditions beyond Earth's atmosphere. However, HEB mixers typically have a limited IF bandwidth between 4–6 GHz [5], in contrast to SIS mixers. Since SIS and HEB receivers on a space-borne satellite are expected to share the same backend microwave spectrometer, the overall bandwidth of the backend receiver chain will therefore be constrained mainly by the available IF bandwidth of HEB mixers. Consequently, unlike ground-based Band 9 mixers designed for ultra-broad IF bandwidth to meet the ALMA-WSU programme, space-borne applications would benefit from broadening the RF bandwidth while maintaining a manageable IF bandwidth e.g., between 8–12 GHz, instead of the more demanding 20 GHz, further mitigating size, weight, and power limitations on the satellite on the backend electronics.

In this section, we refer to the noise-bandwidth requirement of the HSI's Band 1 channel (500–790 GHz), originally proposed for FIRSST [17], as well as the Band 3 channel of SHARP [23], as a guideline for designing our mixer. Fig. 1 depicts the layout of our mixer chip, designed based on two 0.5 μm^2 aluminium oxide (AlO_x) tunnel junctions with a critical current density of about 10 $kAcm^2$, corresponding to a normal-resistance-area (RnA) product of 20 $\Omega\cdot\mu m^2$ and a specific capacitance of 80 $fF/\mu m^2$.

The SIS mixer chip employs a microstrip-fed radial probe antenna [37, 38] positioned across the cross-section of a half-height 100×400 μm rectangular waveguide. The probe antenna is supported on a 10 μm thick silicon-on-insulator (SOI) substrate [39, 40, 41, 34, 42], to facilitates the mounting, alignment, and shaping of the mixer chips. Use of SOI substrate also minimises RF power leakage through the gaps in the trenches hosting the probe antenna mixer chip. The antenna is positioned 96 μm above the waveguide backshort, where the dimensions of the probe and backshort were optimised using HFSS to achieve maximal power coupling over desired bandwidth. Two semi-circular tabs were added to the SOI substrate to accurately positioning the probe relative to the rectangular waveguide [43, 44].

As mentioned earlier, to enhance the power coupling beyond the gap frequency of niobium (0.68 THz), we replace the wiring layer of our mixer circuit with NbTiN, which has a normal sheet resistivity of 200 $\mu\Omega cm^2$ and a critical temperature of $T_c = 15$ K.

Without the need to achieve an ultra-broad IF bandwidth required by ALMA-WSU, we can now utilise a well-controlled microstrip circuit, instead of the earlier CPW designs [36], to enhance flexibility in incorporating various circuit components into our mixer design [1]. The microstrip approach enables a significant broadening of the RF bandwidth by employing a combination of end-stub, end-loaded, and twin-junction [45, 46, 47] tuning methodologies, as shown in the inset of Fig. 1. This improvement is now feasible because achieving the ultra-low impedance sections required for end-stub and/or end-loaded tuning circuits in a CPW configuration is challenging and not compliant with current well-proven photo-fabrication process.

The twin-junction array is embedded in a 400 nm NbTiN top layer and a 250 nm Nb ground

[1]The microstrip RF circuit provides greater flexibility for broadening the RF bandwidth of the chip but inevitably increases the IF capacitance, which limits the IF bandwidth. Hence, the use of CPW transmission lines minimises this parallel-plate capacitance effect, thereby widening the IF bandwidth, as reported in [36].

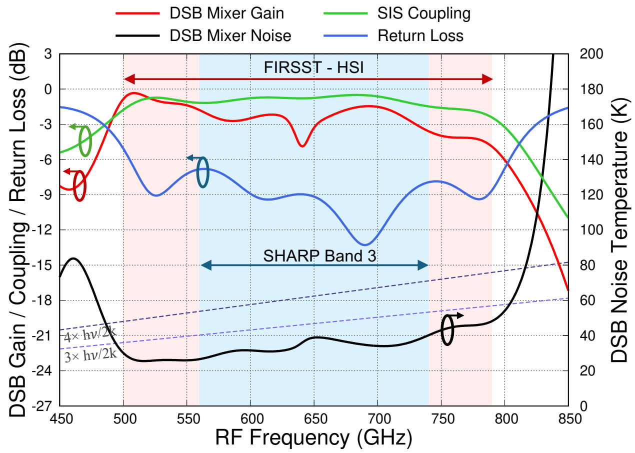

Figure 2: SuperMix-predicted double sideband (DSB) RF noise temperature and conversion gain of the microstrip SIS mixer chip across the FIRSST–HSI Band 1 and SHARP Band 3 ranges, together with the SIS coupling and return loss performance simulated using HFSS.

layer, sandwiching a 250 nm thick silicon monoxide (SiO) dielectric layer forming the microstrip transmission line. A wide microstrip section before the junction array acts as the end-loaded stub, while a secondary wide section connected after the array serves as the end-stub. This end-stub simultaneously functions as part of the tuner circuit and as a microstrip RF choke to prevent RF power leakage into the IF circuitry.

An impedance transformer section is incorporated between the tuner circuit and the microstrip-fed probe antenna to mitigate the impedance mismatch. To reduce parasitic IF capacitance that may still limit the IF bandwidth below 12 GHz, the ground plane beneath the final section of the mixer circuit, where the IF connection beamlead is deposited, was removed, forming a CPW section instead of a microstrip. This modification has minimal impact on RF performance, as the RF circuit is effectively terminated by the RF chokes before this section. Its primary function is simply to provide an electrical connection between the chip and the external IF circuitry. To ensure proper grounding, gold beam leads are deposited along the edges of the mixer chip, and an additional gold beam lead connects the output of the mixer chip directly to the readout circuitry.

We optimised the on-chip circuits using HFSS to maximise the RF power coupling to the SIS junctions, while ensuring the return loss performance is better than -6 dB across the band to avoid potential stability issue during operation. Once the on-chip circuits were finalised, we simulate the heterodyne mixing performance of the mixer chip using SuperMix.

3. RF PERFORMANCE OVER FIRSST-HSI BAND 1

Fig. 2 shows that the predicted mixer performance achieves better than 3× the double-sideband (DSB) quantum-noise limit RF performance from 0.5–0.8 THz, covering the entire FIRSST–HSI Band 1 range (0.5–0.79 THz) as well as SHARP Band 3 (0.56–0.74 THz). Although not highlighted in the plot, the mixer performance also covers the extended Band 9 range proposed by Realini et. al. [35] from 0.58–0.74 THz for the ALMA–WSU programme.

As discussed in [36], the IF performance may vary across RF frequencies and tends to degrade near the RF band edges. This effect is illustrated by the dashed curves in Fig. 3(a), which show the DSB gain and noise performance of the mixer operating at 781 GHz. Notably, the gain declines and the DSB receiver noise increases at higher IF frequencies, although the performance remains below 4× the quantum limit up to about 7 GHz, sufficient to cover the IF bandwidth of HEB mixers for FIR space missions. In Fig. 3(a), we plot the SIS receiver noise-temperature ($T_{\rm rec}$) performance, rather than the intrinsic noise temperature (TN) of the SIS mixer chip, to include the impact of a 3.6 K added noise from the readout low-noise amplifier (LNA) and an additional 5% RF transmission loss from the cold optics, typically mounted at the 20 K stage of a space mission payload. This allows us to demonstrate the influence of the mixer's conversion gain on the overall receiver $T_{\rm rec}$, calculated using

$$T_{\rm rec} = T_{\rm opt}\left(\frac{1}{G_{\rm opt}} - 1\right) + \frac{T_{\rm mix}}{G_{\rm opt}} + \frac{T_{\rm LNA}}{G_{\rm opt}G_{\rm mix}} \quad (1)$$

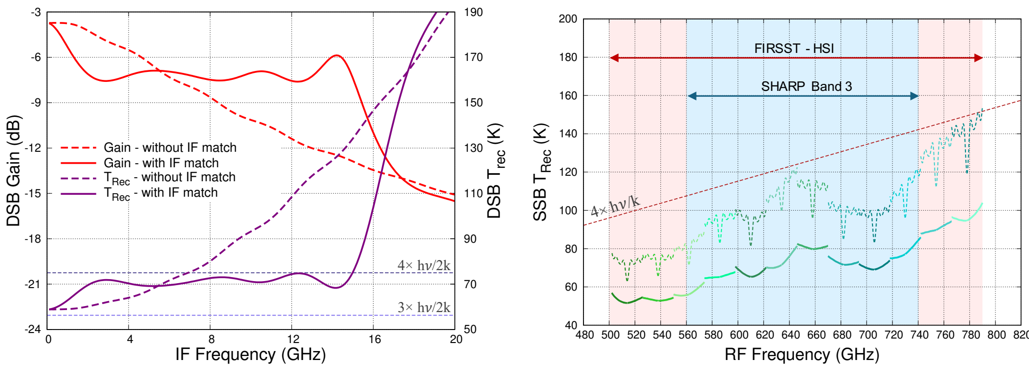

(a) (b)

Figure 3: (a) DSB IF gain and noise temperature performance simulated at 781 GHz. The receiver noise temperature (T_{rec}) prediction includes a readout low-noise amplifier with 3.6 K added noise and a 5% loss from the cold optics, typically anchored at the 20 K physical stage in a space-mission payload module, to account for the effect of the mixer's conversion gain. The solid lines represent the behaviour of the SIS receiver with the IF matching circuit, while the dashed lines represent performance without the IF board. (b) Single-sideband (SSB) noise performance of the microstrip mixer, simulated assuming a readout bandwidth of 12 GHz. The solid lines indicate the intrinsic mixer noise temperature performance, whereas the dashed lines include the noise contribution from the 3.6 K added-noise LNA and an additional 5% optical loss, consistent with panel (a).

where T_{opt} is the physical temperature of the cold optics, $1/G_{\text{opt}}$ the transmission loss of the cold optics, T_{mix} the mixer's intrinsic noise temperature, G_{mix} the mixer's conversion gain, and T_{LNA} the added noise from the LNA.

To enable broader IF bandwidth, we anticipate the use of an external IF matching circuit to enhance IF bandwidth performance, following the design methodology in [48]. As shown by the solid lines in Fig. 3(a), the inclusion of an external IF-matching circuit, typically fabricated using standard printed-circuit-board (PCB) technology, effectively flattens both the DSB gain and noise responses up to approximately 15 GHz.[2]

As shown in Fig. 3(b), this approach enables full coverage of the FIRSST–HSI Band 1 frequency range with only 12 local-oscillator (LO) tunings[3], assuming a 12 GHz readout IF bandwidth with the corresponding LNA[4]. The receiver noise temperature remains below $4 \times h\nu/k$, as required by the mission, even when accounting for a 5% optical loss at the 20 K stage and a 3.6 K readout amplifier added noise. The mixer performance also covers SHARP Band 3, assuming a $4 \times h\nu/k$ noise level. These results demonstrate that the predicted microstrip mixer performance can achieve a significantly wider RF bandwidth than existing ALMA Band 9 mixers while maintaining a respectable 12 GHz IF bandwidth, without relying on hybrid junction technologies (e.g., Nb/NbN or Nb/NbTiN junctions).

4. PERFORMANCE ACROSS LETO BAND 1 REQUIREMENT

Given the promising performance predicted above for an SIS mixer design utilising a NbTiN transmission line and AlO_x-based tunnel junctions near the THz regime, in this section we investigate whether the predicted RF bandwidth performance can be further improved by replacing the AlO_x barrier with aluminium nitride (AlN), while retaining all other materials used in the previously described mixer design. The aim is to broaden the RF bandwidth while maintaining the 12 GHz IF bandwidth, such that the mixer chip can be used to cover both the FIRSST–HSI and the currently proposed ESA–M8 LETO missions, targeting the 0.45–0.82 THz range, as well as both ALMA Band 8 and Band 9, and slightly beyond; a rather demanding requirement for an SIS mixer operating at such high frequencies.

For this investigation, we assume half-micron AlN tunnel junctions with a normal-resistance–area product of $20\,\Omega\cdot\mu\text{m}^2$ and a specific capacitance of $55\,\text{fF}/\mu\text{m}^2$, as reported in [49]. The mixer chip

[2] This limit is primarily due to the large IF capacitance introduced by the on-chip microstrip RF circuits.
[3] The plot assumes a readout IF bandwidth of 0–12,GHz, neglecting the ±0.3,GHz LNA gap for clarity; additional LO tunings would be required to fill these gaps.
[4] Assuming a Low Noise Factory (LNF) 0.3–14,GHz LNA.

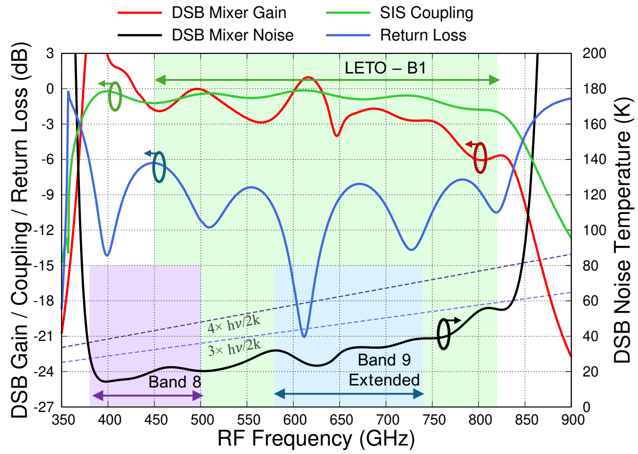

Figure 4: SuperMix predicted double sideband RF noise temperature and conversion gain of the AlN SIS mixer chip across LETO's Band 1, ALMA's Band 8 and extended Band 9 range, and the SIS coupling and return loss performance simulated with HFSS.

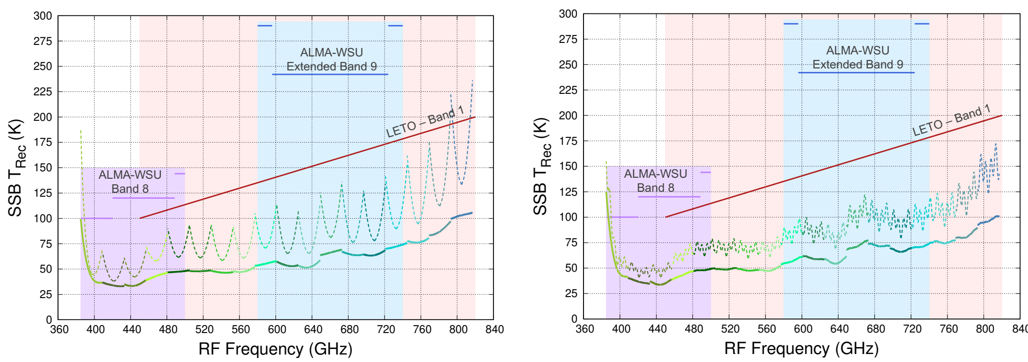

(a) (b)

Figure 5: SSB noise performance of the AlN mixer simulated assuming a readout bandwidth of 12 GHz. The solid lines represent the native mixer noise temperature performance, while the dashed lines include noise contribution from the 3.6 K added noise from the readout LNA and an additional 5% optical loss for cold optics anchored at 20 K stage, taking into account the impact of mixer's conversion gain. The solid horizon/diagonal lines indicate the T_{rec} requirement of ALMA-WSU's Band 8, Band 9 and LETO's Band 1. (a) Without IF matching circuit. (b) With IF matching circuit.

layout follows the earlier design, with optimisations to the probe dimensions and on-chip circuit components tailored to the AlN junctions to maximise RF-bandwidth performance.

Fig. 4 presents the predicted performance of the AlN-based mixer, showing close to 3× DSB noise performance from 0.385–0.825 THz. The return loss performance remains better than –6 dB across this frequency range, indicating that the AlN mixer chip could potentially cover the required bandwidths of the FIRSST–HSI Band 1, SHARP Band 3, LETO Band 1, and the combined ALMA Band 8+9 noise–bandwidth requirements.

We subsequently evaluated the SSB receiver performance of the AlN-based mixer across the target RF bandwidth, as shown in Fig. 5(a). The simulation assumes a 12 GHz readout IF bandwidth in the absence of an external IF matching circuit. The predicted results indicate that the AlN mixer is capable of meeting the noise–bandwidth requirements of LETO Band 1, as well as those of ALMA Band 8 and the extended Band 9 range, even when accounting for 3.6 K of added noise from the readout LNA and an additional 5% optical loss associated with the cold optics anchored at the 20 K stage. The only deviations occur at the lowest 5 GHz segment of ALMA Band 8 and at the uppermost frequency edge of LETO Band 1. As illustrated in Fig. 5(b), the implementation of an external IF matching network, following the methodology outlined in Sec. 3, could further improves the receiver noise temperature, and recovering the sensitivity across the high-frequency end of LETO Band 1. These results demonstrate the feasibility of achieving broad and continuous RF coverage with AlN-barrier SIS mixers while maintaining manageable IF bandwidth, thus satisfying

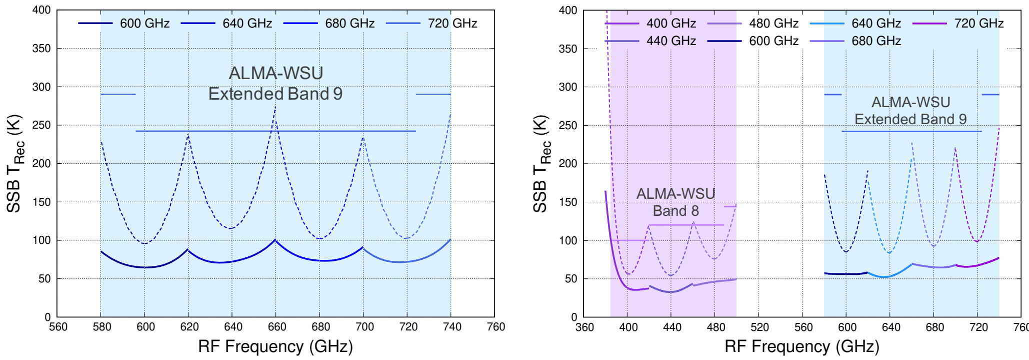

(a) (b)

Figure 6: (a) SuperMix predicted RF and IF bandwidth performance of the microstrip AlO_x mixer. The simulation assumes four LO tunings and a 20 GHz IF readout bandwidth, covering the extended ALMA Band 9 RF range from 0.58–0.74 THz. (b) The RF and IF bandwidth performance of the AlN mixer with seven LO tunings, assuming a 20 GHz IF readout bandwidth, covering both the ALMA's Band 8 (purple shaded area) and the extended Band 9 RF frequency range (light blue shaded area).

the stringent requirements of next-generation far-infrared space observatories.

5. APPLICATION TO ALMA-WSU PROGRAM

The SIS mixer architectures presented above demonstrate performance that approaches the stringent requirements of upcoming FIR space missions, such as FIRSST–HSI, SHARP, and LETO. It is worth noting that the design specifications for space-based FIR missions e.g., those of FIRSST–HSI, are considerably more demanding than those for ground-based observatories such as the ALMA–WSU programme. This distinction is expected, given the reduced optical losses achievable at above-atmosphere observatories, where the optical components are typically cryogenically cooled. Moreover, the extended development and deployment timelines of space missions impose additional constraints, as post-launch instrument upgrades are either impractical or impossible, unlike in ground-based facilities where subsystem enhancements can be implemented on relatively short timescales.

In this context, we examine whether the two SIS mixer architectures presented in this work can also be adapted to the ALMA–WSU programme, which targets substantially broader IF bandwidth coverage near 20 GHz. In this section, we re-simulate the mixer noise–bandwidth performance assuming a 20 GHz IF readout bandwidth, without the inclusion of any external IF-matching circuitry.

Here, we evaluate the performance of the AlO_x-based mixer presented in Sec. 3 across the extended ALMA Band 9 range proposed by [35]. Fig. 6 (a) shows the predicted SSB receiver noise temperature, assuming a 20 GHz readout IF bandwidth and a flat 3.6 K low-noise amplifier (LNA). The results indicate that the design successfully meets the ALMA–WSU-defined 100% noise–bandwidth requirement across the extended Band 9 range (0.58–0.74 THz), as well as the 80% noise–bandwidth requirement from 0.596–0.724 THz, with the exception of a narrow ∼10 GHz gap near 0.66 THz. These results account for a modest 5% optical loss at room temperature (297 K) and a 3.6 K readout-amplifier contribution.

A slight reduction of the IF readout bandwidth to approximately 18 GHz is expected to yield full compliance with the 80% WSU requirement, albeit at the expense of requiring additional LO tunings to recover complete RF coverage. Furthermore, minimising optical losses would enable full compliance with the 80% WSU specification across the entire 100% noise–bandwidth range. The predicted performance also exceeds that of the sub-micron-junction mixer reported in [36], particularly near the RF-band edges, owing to the adoption of a half-height waveguide that enhances probe-antenna coupling and the replacement of Nb with NbTiN, which reduces transmission losses at higher frequencies.

In this section, we evaluate the performance of the AlN-based mixer presented in Sec. 4 to determine whether it can simultaneously satisfy the noise–bandwidth requirements across ALMA Band 8 and the extended Band 9 range, assuming a 20 GHz readout IF bandwidth without the use of an external IF-matching circuit. Fig. 6 (b) presents the predicted SSB receiver noise temperature, including a 5% optical loss referenced to room temperature and a 3.6 K noise contribution from the readout LNA. The results indicate that the AlN mixer largely meets the ALMA–WSU Band 8+9 specifications, with only minor deviations observed at a few frequency points near the lower edge of Band 8. As in previous cases, these residual discrepancies can be mitigated by slightly relaxing the IF readout bandwidth to approximately 18 GHz or by employing additional LO tunings to recover full spectral coverage.

6. CONCLUSION

We have presented the design and simulation study of NbTiN-based SIS mixers employing Nb/AlO_x/Nb and Nb/AlN/Nb tunnel junctions for heterodyne detection in the sub-terahertz frequency range. The proposed microstrip mixer architectures, incorporating end-stub, end-loaded, and twin-junction tuning networks, demonstrate the capability to achieve simultaneously broad RF and practical IF bandwidths while maintaining receiver noise temperatures within three to four times the quantum limit. Depending on the specific requirements of future FIR space missions, either of the two mixer designs shows the potential to meet the stringent noise–bandwidth criteria of upcoming space-based observatories. Although originally developed for space-borne applications, the same SIS mixer architectures are equally applicable to ground-based observatories, such as the ALMA–WSU programme.

ACKNOWLEDGMENT

This research was funded in part by the European Commission Horizon-Infra-2022-Tech-01 RadioBlock project, and the UK-STFC Small Award 2024 Grant (ST/Y002210/1).

REFERENCES

1. R. Blundell and D. Winkler, "The superconductor insulator superconductor mixer receiver—a review," *Nonlinear Superconductive Electronics and Josephson Devices*, pp. 55–72, 1991.
2. V. Belitsky, S. Cherednichenko, and D. Winkler, "Low-noise superconducting mixers for the terahertz frequency range," in *Handbook of Superconductivity*. CRC Press, 2022, pp. 797–811.
3. M. Tarenghi, "The atacama large millimeter/submillimeter array: overview & status," *Astrophysics and Space Science*, vol. 313, no. 1, pp. 1–7, 2008.
4. G. H. Tan, "The alma front ends: an overview," in *Proc. 19th Int. Symp. Space Terahertz Technol*, 2008.
5. W. Zhang, W. Miao, Y. Ren, K.-M. Zhou, and S.-C. Shi, "Superconducting hot-electron bolometer mixers and their applications," *Superconductivity*, vol. 2, p. 100009, 2022.
6. B.-L. Liu, D. Liu, M. Yao, J.-D. Jin, Z. Wang, J. Li, S.-C. Shi, A. Chekushkin, M. Fominsky, L. Filippenko *et al.*, "Terahertz high-sensitivity sis mixer based on nb–aln–nbn hybrid superconducting tunnel junctions," *Chinese Physics B*, vol. 33, no. 5, p. 058501, 2024.
7. K. I. Rudakov, F. V. Khan, A. Chekushkin, A. Khudchenko, V. Koshelets *et al.*, "Sub-thz range superconducting sis receivers for space and ground-based radio astronomy," *Technical Physics*, vol. 69, no. 7, pp. 1011–1017, 2024.
8. I. V. Tretyakov, A. V. Khudchenko, K. I. Rudakov, I. V. Ivashentseva, N. S. Kaurova, B. M. Voronov, M. S. Kirsanova, T. I. Larchenkova, G. N. Goltsman, A. M. Baryshev *et al.*, "Development of mixers for the high resolution spectrometer of the millimetron space observatory," *IEEE Transactions on Terahertz Science and Technology*, 2024.
9. J. L. Pineda, J. V. Siles, J. Kawamura, W. D. Langer, P. F. Goldsmith, D. C. Lis, P. Bernasconi, C. Groppi, L. Anderson, C. Battersby *et al.*, "The Far-Infrared Astronomy Stratospheric Balloon Facility," *Bulletin of the American Astronomical Society*, pp. 7–177, 2019.
10. P. F. Goldsmith, "Stratospheric Balloon Missions for High Resolution Submillimeter-FIR Astronomical Spectroscopy," in *2023 48th International Conference on Infrared, Millimeter, and Terahertz Waves (IRMMW-THz)*. IEEE, 2023, pp. 1–2.
11. E. Udinski and A. Hamilton, "2024 NASA Balloon Program Overview," in *JAXA and Hiroshima University Collaboration Meetings*, 2024.
12. J. R. Silva, C. Walker, C. Kulesa, A. Young, J.-R. Gao, Q. Hu, J. Hesler, A. Emrich, P. Hartogh, W. Laauwen *et al.*, "High-resolution receiver for the single aperture large telescope for universe studies," *Journal of Astronomical Telescopes, Instruments, and Systems*, vol. 10, no. 4, pp. 042 308–042 308, 2024.

13. D. Rigopoulou, M. Caldwell, B. Ellison, C. Pearson, E. Caux, A. Cooray, J. Gallego, M. Gerin, J. Goicoechea, P. Goldsmith *et al.*, “The Far Infrared Spectroscopic Explorer (FIRSPEX): probing the lifecycle of the ISM in the universe,” in *Space Telescopes and Instrumentation 2016: Optical, Infrared, and Millimeter Wave*, vol. 9904. SPIE, 2016, pp. 850–856.
14. I. Mehdi, P. Goldsmith, D. Lis, J. Pineada, B. Langer, J. Siles, J. Kawamura, B. Karasik, G. Chattopadhay, J. Pearson *et al.*, “Far-infrared heterodyne array receivers,” *Bulletin of the American Astronomical Society*, vol. 51, no. 7, pp. id–120, 2019.
15. D. Rigopoulou, C. Pearson, B. Ellison, M. Wiedner, V. O. Okada, B. Tan, I. Garcia-Bernete, M. Gerin, G. Yassin, E. Caux *et al.*, “The far-infrared spectroscopic surveyor (FIRSS),” *Experimental Astronomy*, vol. 51, no. 3, pp. 699–728, 2021.
16. D. Rigopoulou, B. K. Tan, B. Ellison, C. Pearson, S. Aalto, E. Caux, I. Garcia-Bernete, M. Gerin, J. R. Goicoechea, P. Goldsmith *et al.*, “The far-infrared spectroscopic surveyor: probing role of the interstellar medium in star formation and galaxy evolution,” in *Space Telescopes and Instrumentation 2022: Optical, Infrared, and Millimeter Wave*, vol. 12180. SPIE, 2022, p. 121802G.
17. M. C. Wiedner, A. Baryshev, P. Grimes, and B. Tan, “Concept study of the Heterodyne Spectroscopy Instrument (HSI) for the proposed Far-IR Spectroscopy Space Telescope (FIRSST),” in *Proceedings of the 34th IEEE International Symposium on Space THz Technology.* National Radio Astronomy Observatory, 2024.
18. D. e. a. Rigopoulou, “Light emission terahertz observatory (leto): A european space agency m8 mission proposal,” unpublished.
19. F. Roelofs, C. M. Fromm, Y. Mizuno, J. Davelaar, M. Janssen, Z. Younsi, L. Rezzolla, and H. Falcke, “Black hole parameter estimation with synthetic very long baseline interferometry data from the ground and from space,” *Astronomy & Astrophysics*, vol. 650, p. A56, 2021.
20. N. Patel, M. Johnson, T. Norton, S. Doeleman, M.-T. Chen, C.-C. Han, S. Matsushita, K. Asada, P. Ho, U.-L. Pen *et al.*, “Planned upgrades on the Greenland Telescope for the Next Generation Event Horizon Telescope observations,” in *American Astronomical Society Meeting Abstracts*, vol. 55, 2023, pp. 305–16.
21. R. Evans, “The africa millimetre telescope,” *High Energy Astrophysics in Southern Africa*, p. 45, 2021.
22. C. E. Tong, K. Akiyama, P. Grimes, M. Honma, J. Houston, M. D. Johnson, D. P. Marrone, H. Rana, and Y. Uzawa, “Receivers for the black hole explorer (bhex) mission,” in *Space Telescopes and Instrumentation 2024: Optical, Infrared, and Millimeter Wave*, vol. 13092. SPIE, 2024, pp. 2212–2218.
23. E. e. a. Villard, “Space-based high-resolution array for radio astronomy and physics (sharp): A european space agency m8 mission proposal,” unpublished.
24. S. Asayama, G. Tan, K. Sini *et al.*, “Report of the alma front-end & digitizer requirements upgrade working group,” *ALMA Report*, 2020.
25. J. Carpenter, C. Brogan, D. Iono, and T. Mroczkowski, “The alma2030 wideband sensitivity upgrade,” *arXiv preprint arXiv:2211.00195*, 2022.
26. M. Booth, P. Klaassen, C. Cicone, T. Mroczkowski, M. A. Cordiner, L. Di Mascolo, D. Johnstone, E. van Kampen, M. M. Lee, D. Liu *et al.*, “Atlast science overview report,” *arXiv preprint arXiv:2407.01413*, 2024.
27. R. Kawabe, K. Kohno, Y. Tamura, T. Takekoshi, T. Oshima, and S. Ishii, “New 50-m-class single-dish telescope: Large submillimeter telescope (lst),” in *Ground-based and Airborne Telescopes VI*, vol. 9906. SPIE, 2016, pp. 779–790.
28. L. He, F. Lin, and X. He, “Design of waveguide nbn-based superconductor–insulator–superconductor mixer for 650 ghz,” *Advanced Photonics Research*, p. 2400197, 2025.
29. N. V. Kinev, A. M. Chekushkin, F. V. Khan, K. I. Rudakov, N. Kotova, and V. P. Koshelets, “Study of superconducting transmission lines based on nbtin/al and pumping of nb/aln/nbn sis junctions in the frequency range above 1 thz,” *Physics of the Solid State*, vol. 66, no. 7, pp. 1000–1005, 2024.
30. A. Khudchenko, A. M. Baryshev, K. I. Rudakov, P. M. Dmitriev, R. Hesper, L. de Jong, and V. P. Koshelets, “High-gap nb-aln-nbn sis junctions for frequency band 790–950 ghz,” *IEEE Transactions on Terahertz Science and Technology*, vol. 6, no. 1, pp. 127–132, 2015.
31. I. Ansys, “Ansys engineering simulation software.” [Online]. Available: http://https://www.ansys.com/en-gb

32. J. Ward, F. Rice, G. Chattopadhyay, and J. Zmuidzinas, "SuperMix: A flexible software library for high-frequency circuit simulation, including SIS mixers and superconducting elements," in *Proceedings, Tenth International Symposium on Space Terahertz Technology*, pp. 269–281.
33. F. R. Rice, *A Very Wide Bandwidth SIS Heterodyne Receiver Design for Millimeter and Submillimeter Astronomy.* California Institute of Technology, 2020.
34. B.-K. Tan, G. Yassin, P. Grimes, K. Jacobs, and S. Withington, "Preliminary measurement results of a 650 GHz planar circuit balanced SIS mixer," *IEEE Transactions on Terahertz Science and Technology*, vol. 3, no. 1, pp. 32–38, 2013.
35. S. Realini, R. Hesper, J. Barkhof, and A. Baryshev, "ALMA Band 9 upgrade: a feasibility study," in *EPJ Web of Conferences*, vol. 293. EDP Sciences, 2024, p. 00043.
36. B. Tan, J. Kim, C. Chaumont, F. Boussaha, and A. Baryshev, "Analysing the RF & IF bandwidth performances of ALMA Band-9 superconducting mixers for wideband sensitivity upgrade," *Superconductor Science and Technology*, vol. 38, no. 8, p. 085001, 2025.
37. S. Withington, J. Leech, G. Yassin, K. Isaak, B. Jackson, J. Gao, and T. Klapwijk, "A 350ghz radial-probe sis mixer for astronomical imaging arrays," *International Journal of Infrared and Millimeter Waves*, vol. 22, no. 9, pp. 1305–1312, 2001.
38. J. Kooi, G. Chattopadhyay, S. Withington, F. Rice, J. Zmuidzinas, C. Walker, and G. Yassin, "A full-height waveguide to thin-film microstrip transition with exceptional RF bandwidth and coupling efficiency," *International Journal of Infrared and Millimeter Waves*, vol. 24, no. 3, pp. 261–284, 2003.
39. A. B. Kaul, B. Bumble, K. A. Lee, H. G. LeDuc, F. Rice, and J. Zmuidzinas, "Fabrication of wide-IF 200–300 GHz superconductor–insulator–superconductor mixers with suspended metal beam leads formed on silicon-on-insulator," *Journal of Vacuum Science & Technology B: Microelectronics and Nanometer Structures Processing, Measurement, and Phenomena*, vol. 22, no. 5, pp. 2417–2422, 2004.
40. M. Westig, K. Jacobs, J. Stutzki, M. Schultz, M. Justen, and C. Honingh, "Balanced superconductor–insulator–superconductor mixer on a 9 μm silicon membrane," *Superconductor Science and Technology*, vol. 24, no. 8, p. 085012, 2011.
41. B.-K. Tan, G. Yassin, P. Grimes, and K. Jacobs, "650 GHz SIS mixer fabricated on silicon-on-insulator substrate," *Electronics letters*, vol. 49, no. 20, pp. 1273–1275, 2013.
42. B. Tan, G. Yassin, P. Grimes, and K. Jacobs, "Designs of broadband unilateral finline sis mixers employing 15 μm silicon-on-insulator substrate at THz frequencies," in *International Symposium on Space Terahertz Technology.* National Radio Astronomy Observatory, 2010.
43. B. Tan, K. Rudakov, V. Koshelets, A. Khudchenko, A. Baryshev, and G. Yassin, "Comparing the performance of 850 GHz integrated bias-tee superconductor-insulator-superconductor (SIS) mixers with single-and parallel-junction tuner," *Superconductor Science and Technology*, vol. 35, no. 12, p. 125008, 2022.
44. B.-K. Tan, K. Rudakov, V. P. Koshelets, A. Khudchenko, A. M. Baryshev, and G. Yassin, "Electromagnetic performance comparisons of 0.85 THz integrated bias-tee SIS mixers with twin-junction and end-loaded tuning schemes," in *Millimeter, Submillimeter, and Far-Infrared Detectors and Instrumentation for Astronomy XI*, vol. 12190. SPIE, 2022, pp. 868–873.
45. B. K. Tan, *Development of coherent detector technologies for sub-millimetre wave astronomy observations.* Springer, 2015.
46. J. Zmuidzinas, H. G. LeDuc, J. A. Stern, and S. R. Cypher, "Two-junction tuning circuits for submillimeter SIS mixers," *IEEE transactions on microwave theory and techniques*, vol. 42, no. 4, pp. 698–706, 1994.
47. V. Y. Belitsky, S. Jacobsson, L. Filippenko, and E. Kollberg, "Broadband twin-junction tuning circuit for submillimeter SIS mixers," *Microwave and Optical Technology Letters*, vol. 10, no. 2, pp. 74–78, 1995.
48. B.-K. Tan, G. Yassin, and P. Grimes, "Ultra-wide intermediate bandwidth for high-frequency SIS mixers," *IEEE Transactions on Terahertz Science and Technology*, vol. 4, no. 2, pp. 165–170, 2014.
49. A. Pavolotsky, T. Kojima, S. Masui, and V. Belitsky, "SIS technology development to serve Next Generation receivers for ALMA," in *Proceedings of the 32nd IEEE International Symposium on Space THz Technology (ISSTT 2022)*, 2022, pp. 16–20.